



The N-terminal 14-mer model peptide of human Ctr1 can collect Cu(II) from albumin. Implications for copper uptake by Ctr1

Journal:	<i>Metallomics</i>
Manuscript ID	MT-COM-09-2018-000274.R2
Article Type:	Communication
Date Submitted by the Author:	09-Nov-2018
Complete List of Authors:	<p>Stefaniak, Ewelina; Polish Academy of Sciences, Institute of Biochemistry and Biophysics Płonka, Dawid; Polish Academy of Sciences, Institute of Biochemistry and Biophysics Drew, Simon; Department of Medicine, Royal Melbourne Hospital, University of Melbourne Bossak-Ahmad, Karolina; Polish Academy of Sciences, Institute of Biochemistry and Biophysics Haas, Kathryn ; Saint Mary's College, Department of Chemistry and Physics Pushie, M.; University of Saskatchewan, College of Medicine Faller, Peter; Institut de Chimie de Strasbourg, UMR 7177 Wezynfeld, Nina; Institut de Chimie de Strasbourg, UMR 7177; Polish Academy of Sciences, Institute Biochemistry and Biophysics Bal, Wojciech; Polish Academy of Sciences, Institute of Biochemistry and Biophysics</p>

Journal Name

COMMUNICATION

The N-terminal 14-mer model peptide of human Ctr1 can collect Cu(II) from albumin. Implications for copper uptake by Ctr1

Received 00th January 20xx,
Accepted 00th January 20xx

Ewelina Stefaniak,^a Dawid Płonka,^a Simon C. Drew,^b Karolina Bossak-Ahmad,^a Kathryn L. Haas,^c M. Jake Pushie,^d Peter Faller,^e Nina E. Wezinfeld,^{*a,e} and Wojciech Bal^{*a}

DOI: 10.1039/x0xx00000x

www.rsc.org/

Human cells acquire copper primarily via the copper transporter 1 protein, hCtr1. We demonstrate that at extracellular pH 7.4 Cu^{II} is bound to the model peptide hCtr1₁₋₁₄ via an ATCUN motif and such complexes are strong enough to collect Cu^{II} from albumin, supporting the potential physiological role of Cu^{II} binding to hCtr1.

Significance to metallomics

Copper import to cells is necessary for many intracellular processes driven by copper-dependent enzymes. Dysregulation of this homeostasis could lead to various diseases, including Alzheimer's and Parkinson's diseases. Human copper transporter 1, hCtr1, has been identified as the main copper transporter for human cells. However, the precise mechanism of copper import to the cells remains unsolved. Our studies provide the first experimental evidence that the N-terminus of hCtr1 can collect Cu^{II} from albumin, one of the main Cu^{II} carriers in blood. The direct transfer of Cu^{II} from albumin to hCtr1 is the likely first step of Cu^{II} acquisition by human cells.

Copper (Cu) is crucial for a number of key human enzymes, involved in mitochondrial respiration, antioxidant defence, and neurotransmitter biosynthesis.¹ However, in excess Cu is also toxic, causing production of reactive oxygen species (ROS) and promoting oligomerization of proteins and peptides, known as toxic processes for neurodegenerative diseases such as Alzheimer's and Parkinson's diseases.^{2,3} Therefore, the process

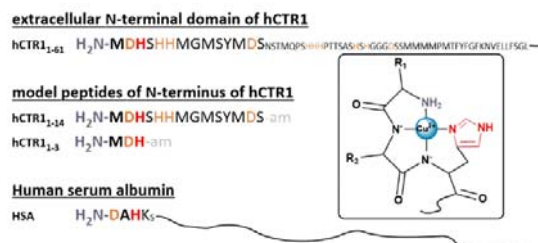


Fig. 1. The sequence of extracellular N-terminal domain of human copper transporter 1 hCtr1, a model peptide of hCtr1 used in this study, hCtr1₁₋₁₄, a model peptide of hCtr1 used in the previous study, hCtr1₁₋₃, and the N-terminal sequence of human serum albumin. The insert shows Cu^{II} bound to the ATCUN motif. The His3 and the N-terminal amine crucial for this type of Cu^{II} coordination are highlighted in red and grey, respectively. Other residues that could participate in the Cu^{II} binding are orange.

of cellular Cu acquisition, together with its distribution and storage have to be tightly controlled.

Human copper transporter 1 (hCtr1) is the main protein responsible for Cu import into cells. The protein is localized to the plasma membrane and possesses three membrane spanning domains. The protein homotrimerizes to create a cone shaped pore.⁴ The hCtr1 protein acquires Cu from the extracellular space, where Cu exists primarily in the Cu^{II} oxidation state. It is proposed that Cu^{II} bound to the extracellular domain is reduced by small-molecule reducing agents.⁵ The Cu atom is then passed through a Cu^I selectivity filter, formed from a conserved and essential MXXXM sequence in the second transmembrane domain,⁶ and is delivered to cytoplasmic Cu chaperone proteins, including Atox1.⁷ The chemical details of Cu acquisition and its translocation into the cytoplasm are not well understood. The N-terminal extracellular domain of hCtr1 contains multiple methionine- and histidine-rich motifs that are anchoring sites for Cu^I and Cu^{II} ions (Fig. 1) and that are important for high-affinity Cu acquisition of hCtr1 in tissue culture models.^{8,9} In cell culture studies the truncation of the extracellular N-terminal domain of hCtr1 resulted in the significant decrease of copper import.^{10,11} These experiments support a crucial role for the extracellular

^a Institute of Biochemistry and Biophysics, Polish Academy of Sciences, Pawińskiego 5a, 02-106 Warsaw, Poland. E-mail: nina@ibb.waw.pl, wbal@ibb.waw.pl

^b Department of Medicine, Royal Melbourne Hospital, University of Melbourne, Melbourne, VIC 3010, Australia

^c Department of Chemistry and Physics, Saint Mary's College, Notre Dame, Indiana 46556, United States

^d Department of Surgery, Division of Neurosurgery, College of Medicine, University of Saskatchewan, 107 Wiggins Road, Saskatoon, Saskatchewan S7N 5E5, Canada.

^e Institut de Chimie, UMR 7177, CNRS-Universite' de Strasbourg, 4 rue Blaise Pascal, Strasbourg, 67000, France.

Electronic Supplementary Information (ESI) available: Experimental procedures, calculated Vis and CD spectra of complexes, EPR results. See DOI: 10.1039/x0xx00000x

domain of hCtr1 and particularly its Cu-binding motifs in effective hCtr1 Cu acquisition.

Mammalian Ctr1 proteins, including hCtr1, also possess the Amino Terminal Cu^I- and Ni^{II}-binding site (ATCUN), characterized by the general sequence H₂N-Xaa-Zaa-His spanning the first three protein residues. The Cu^{II} ion is bound there via the N-terminal amine, the first two amides, and the imidazole of His3 (4N, Fig. 1), reaching nearly femtomolar Cu^{II} affinities at pH 7.4.^{12–14}

Such strong binding suggests a potential role of ATCUN Cu^{II} complexes in copper cellular import, which is different from the mechanism known in yeast, where Cu^{II} is reduced to Cu^I by a complimentary Cu reductase prior to its binding to yeast Ctr1.¹⁵ The presence of a Cu^{II}-specific binding site in the extracellular domain of hCtr1 may also facilitate the direct shuttling of Cu^{II} ions from extracellular ligands, including Human Serum Albumin (HSA), one of the main Cu^{II} carriers in the blood.¹⁶ Studies on cell cultures showed that radioactive ⁶⁴Cu^{II} loaded to albumin can be acquired by cells.¹⁷ Furthermore, EPR experiments on spin-labelled hCtr1_{1–14}, and HSA indicated a close interaction between these molecules.¹⁸ Considering Cu acquisition as a process involving hCtr1 and HSA, one can consider two non-exclusive possibilities (i) a direct Cu^{II} transfer from HSA to hCtr1 or (ii) the reduction of Cu^{II} prior to the binding to hCtr1.¹⁹ The presence of the ATCUN in the hCtr1 sequence favours the former mechanism. However, HSA also contains the ATCUN motif and should also display high affinity for Cu^{II}. Cu^{II} affinities of previously studied model peptides hCtr1_{1–55} and hCtr1_{1–14}, ^cK_{7,4}=2.6×10⁸ and 1×10¹¹ M⁻¹, respectively,^{8,20} are much lower than that reported for HSA, ^cK_{7,4}=1×10¹² M⁻¹ at pH 7.4.²¹ The stronger affinity of the HSA ATCUN site brings the transfer of Cu^{II} ions from HSA to hCtr1 into question. Contrary to these reported affinities, a recent study of Cu^{II} binding to hCtr1_{1–3} yielded the rigorously established ^cK_{7,4}=1.3×10¹³ M⁻¹, being the first piece of data supporting a stronger affinity for the hCtr1 ATCUN site, and thus a rationalization for a thermodynamically favourable Cu^{II} transfer from HSA to

Table 1. Protonation and stability constants (logβ values) for hCtr1_{1–14} (L) and its Cu^{II} complexes at I = 0.1 m (KNO₃) and 25 °C. Standard deviations on the last digits are given in parentheses. See text for description of coordination modes.

Species	Logβ	pK	Assignment	Coordination mode
H ₇ L	43.20(1)	2.92	Asp2/13	
H ₆ L	40.27(1)	4.03	Asp2/13	
H ₅ L	36.24(1)	5.78	His3/5/6	
H ₄ L	30.46(1)	6.23	His3/5/6	
H ₃ L	24.23(1)	6.93	His3/5/6	
H ₂ L	17.30(1)	7.46	N ^{am} of Met1	
HL	9.84(1)	9.84	Tyr11	
CuH ₄ L	35.37(2)		N ^{am} of Met1, His3, Asp2	2N2O
CuH ₃ L	31.62(1)	3.67	Asp13	2N2O
CuH ₂ L	27.04(1)	4.46	N, N', reprot. Asp2/13	4N*
CuHL	21.64(1)	4.88	redeprot. Asp2/13	4N*
CuL	15.37(1)	5.85	His5/6	4N
CuH ₁ L	8.25(1)	6.84	His5/6	4N
CuH ₂ L	-1.74(1)	10.04	Tyr11	4N

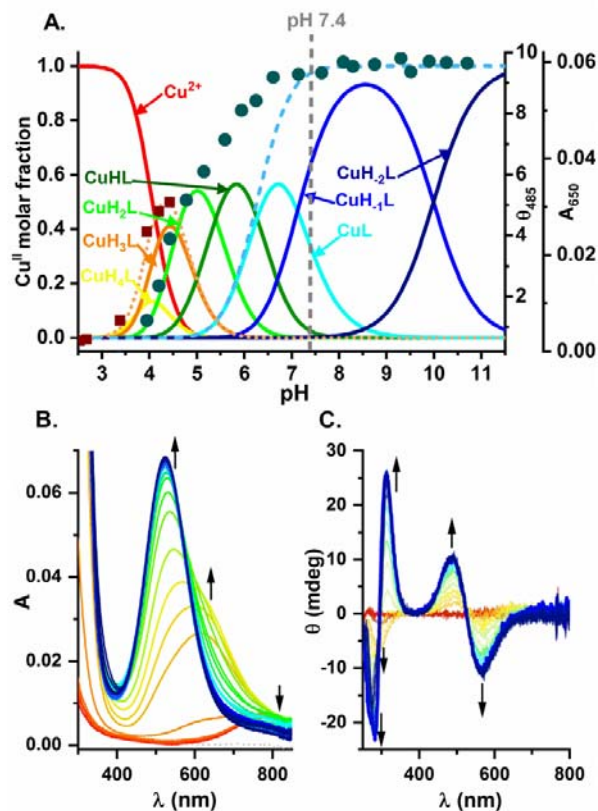


Fig. 2. pH dependence of the formation of Cu^{II} complexes with hCtr1_{1–14} model peptide (MDHSHHMGMSYMDS-am) (A) Species distributions of Cu^{II} complexes of hCtr1_{1–14}, calculated for concentrations used in UV-vis and CD titrations (0.6 mM peptide and 0.5 mM Cu^{II}) using stability constants from Table 1. The common scale left-side axes represent Cu^{II} molar fractions. Cu^{II} species are color-marked as described in the Figure. The orange dotted line shows the sum of 2N2O complexes and a blue dashed line the sum of 4N complexes (ML, MH₁L, MH₂L). The right-side axes provide absorbance, and ellipticity obtained in spectroscopic experiments: brown squares, A₆₅₅; blue circles θ₄₈₅. UV-vis (B) and CD (C) titrations of the solution of 0.6 mM hCtr1_{1–14} and 0.5 mM Cu^{II} coded with rainbow colors from red (the lowest pH 2.1) to navy (the highest pH 11.5). The directions of spectral changes are marked by arrows.

hCtr1.²² The minimalism of the hCtr1_{1–3} model, which contained only three first amino acids necessary to create the ATCUN motif, may not sufficiently reproduce the Cu^{II} binding properties of the hCtr1 domain. Further, the previously-determined affinities of hCtr1_{1–14} and hCtr1_{1–55} peptides for Cu^{II} were reported as conditional values and explicitly did not account for the interference of buffer and other solution components.^{8,20} Therefore, we decided to re-evaluate the Cu^{II} affinity of the 14 amino acid peptide in the absence of interfering solution components. This hCtr1_{1–14} peptide is expected to perform as a better model of the extracellular N-terminus of hCtr1 than hCtr1_{1–3} due to the presence of additional Cu-binding groups that are adjacent to the ATCUN site, including His5, His6, and Asp13 (see Fig. 1 for sequences). We also attempted to estimate the rate of Cu^{II} transfer from HSA to hCTR1_{1–14}.

We employed potentiometry to obtain pK_a values of the hCtr1_{1–14} residues, which are presented in Table 1. The Asp

residues released the proton at the most acidic pH, with an average of pK_a 3.5 ± 0.6 , followed by His residues, with an average pK_a of 6.3 ± 0.6 . These values are consistent with previously reported data for these residues in other peptides.^{23,24} The N-terminal amino group is deprotonated with a typical pK_a , very similar to that in hCtr1₁₋₃.²² As expected from previous studies of tyrosine-containing peptides, the highest pK_a 9.8 was determined for Tyr11.^{14,23,24}

The pH dependence of Cu^{II} binding to hCtr1, presented in Fig. 2, revealed that all coordination changes occur below pH 7.4. After the formation of CuL species, at neutral and basic pH the ATCUN 4N coordination mode dominates, as evidenced by its spectral parameters presented in Supporting Information, Table S1. They are in a good agreement with those obtained for the hCtr1₁₋₃ peptide.²² Further deprotonations of one of the His residues (His5/6) and Tyr11 (formation of CuH₁LH and CuH₂L species, respectively) did not influence the Cu^{II} coordination. Thus, just the first three amino acids are responsible for Cu^{II} binding at pH 7.4. This pH is characteristic for the extracellular space, where the N-terminal domain of hCtr1 is mainly present due to the exclusive localization of hCtr1 in the plasma membrane.²⁵ As a consequence, the Cu^{II}-ATCUN complex is likely to be the principle physiological form of Cu^{II}-hCtr1.

hCtr1 has been found to be localized also in the intracellular compartments including lysosomes,²⁵ where pH is acidic, even lower than 5.²⁶ Our experiments revealed that Cu^{II} coordination to hCtr1₁₋₁₄ can be different at this pH. From pH 3.2–4.6, two 2N2O species, represented by CuH₄L and CuH₃L, are the dominant Cu^{II}-hCtr1₁₋₁₄ species. The N-terminal amine, the His3 imidazole, and the Asp2 carboxylate oxygen participate in the Cu^{II} binding in these species. The Cu^{II} coordination sphere is complemented either by H₂O (CuH₄L with Asp13 protonated and CuH₃L with Asp13 deprotonated) or by deprotonated Asp13 carboxylate (for CuH₃L). The calculated spectra of these species support this coordination (the UV-vis d-d band λ_{max} at 610 nm and the negative CD band at 299 nm, see Supporting Information Fig. S1 and Table S1).²⁷

Then, between pH 4.6–6.3, CuH₂L and CuHL are the most abundant Cu^{II} species. Their spectra were significantly overlapped with those of other complexes, therefore potentiometric results were used to deconvolute them to establish the coordination mode(s). The obtained spectra of CuH₂L and CuHL species were identical to each other and significantly similar to the spectra of 4N complexes at pH above 7.4 (see Supporting Information Fig. S1), meaning that they were generated by the same ATCUN motif. However, slight changes in λ_{max} and a noticeably lower intensity of the CuH₂L and CuHL spectra compared to previously described 4N complexes at basic conditions result probably due to interactions in the second coordination sphere. Therefore, we distinguished Cu^{II}-ATCUN complexes at basic and acidic conditions, calling them 4N (CuL, CuH₁L, CuH₂L) and 4N* (CuH₂L, CuHL), respectively.

Despite the fact that the first three amino acid (ATCUN) residues are mostly responsible for Cu^{II} binding to hCtr1₁₋₁₄ around pH 7.4, the downstream residues could affect the affinity of this complex. The close similarity of $K_{7,4}$ value calculated here for

hCtr1₁₋₁₄ with that reported for Cu^{II}-hCtr1₁₋₃, $1.0 \times 10^{13} \text{ M}^{-1}$ vs. $1.3 \times 10^{13} \text{ M}^{-1}$ indicates that the impact of His5, His6 or Asp13 on the affinity of the N-terminus of hCtr1 to Cu^{II} is very minor at the pH of the extracellular space. The binding constant obtained in this study for hCtr1₁₋₁₄ is higher than that obtained previously for the same model peptide, hCtr1₁₋₁₄, by the competition with NTA in a 50 mM HEPES buffer.⁸ HEPES is a weak Cu^{II} chelator.²⁸ It affects the stability constant determination by lowering the free Cu²⁺ concentration and by increasing the apparent Cu^{II} affinity of NTA *via* ternary complex formation.²¹ These effects were not included in the previous analysis. By taking them into account we calculated a correction factor of 2.24 log units, elevating the recalculated log K value from ref. 7 from 11.0 ± 0.3 to 13.2 ± 0.3 , in a perfect match with the potentiometric result, 13.0 ± 0.01 in log units.

The affinity constant calculated in this study for Cu^{II}-hCtr1₁₋₁₄ is 10 times higher than that reported for Cu^{II}-HSA at pH 7.4, in principle enabling the Cu^{II} transfer from HSA to hCtr1. To prove experimentally that this process can occur, we employed CD spectroscopy to monitor the interaction between Cu^{II}-HSA²¹ and hCtr1₁₋₁₄, based on differences in intensities of the CT and d-d bands for Cu^{II}-HSA and Cu^{II}-hCtr1₁₋₁₄. As shown in Fig. 3, the addition of hCtr1₁₋₁₄ to Cu^{II}-HSA caused the increase of intensity of these bands. It resulted in the formation of Cu^{II}-hCtr1₁₋₁₄ as bands of Cu^{II}-hCtr1₁₋₁₄ are more intense compared to those of Cu^{II}-HSA. The $t_{1/2}$ value of 16.2 ± 0.8 min, as well as the transfer degree of about 90% calculated for this process are consistent with the difference of affinities of the respective Cu^{II} complexes. The direct Cu^{II} transfer from HSA to hCtr1₁₋₁₄ in a similar time scale and with no intermediate species was also independently confirmed by EPR (see Supporting Information Fig. S2).

To the best of our knowledge, these results provide the first experimental evidence that HSA can directly deliver Cu^{II} to the model peptide of the hCtr1 N-terminus. Previously, only suggestions were made, based on the comparison of Cu^{II} affinities of HSA and peptide models of hCtr1²² or studies on

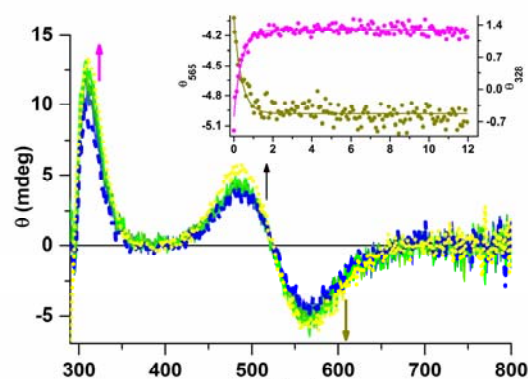


Fig. 3. CD monitored reaction between Cu^{II} bound to the ATCUN motif of human serum albumin and the hCtr1₁₋₁₄ model peptide (MDHSHHMGMSYMDS-am). The spectra were collected every 5 min and their time order is coded with solid blue to green lines. The spectra of Cu^{II}(HSA) and Cu^{II}(hCtr1₁₋₁₄) are marked by dashed blue and dotted yellow lines, respectively. The insert represents the kinetics of the studied reaction monitored by changes of the intensities for the selected signals at 328 nm and 556 nm. The reaction was performed for 0.4 mM concentration of HSA and hCtr1₁₋₁₄ related to the ATCUN motif and 0.32 mM of CuCl₂ in 50 mM HEPES, pH 7.4.

interactions between HSA and hCtr1 model peptides, but in the absence of Cu^{II}.¹⁸

Extended X-ray absorption fine structure (EXAFS) spectroscopy of Cu^{II} bound to HSA, and hCtr1₁₋₁₄ at pH 7.4 reveals that their coordination environment is subtly different, as evidenced by the EXAFS spectrum (Fig. 4 inset) and Fourier transform (Fig. 4). While this data supports that both molecules bind Cu^{II} through ATCUN coordination and our results are in agreement with other EXAFS spectra reported for this type of Cu^{II} complexes,^{29,30} the subtle difference in coordination environment between HSA, and hCtr1₁₋₁₄ further supports the observed difference in their Cu^{II} binding affinities. The average Cu^{II}-N distance for the 4N core is 1.96 Å.

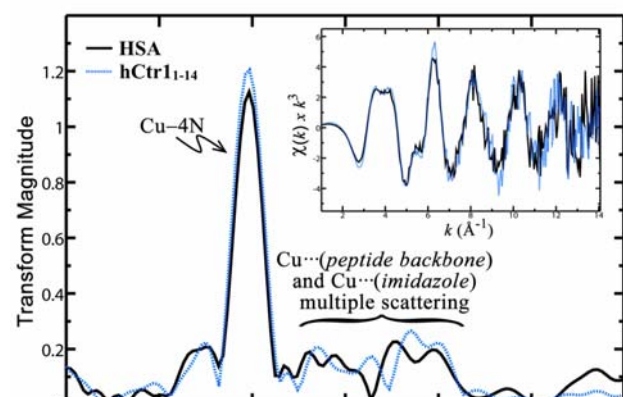


Fig. 4. EXAFS spectrum (inset) and EXAFS Fourier transform of Cu^{II} bound to HSA (black line), and Cu^{II} bound to hCtr1₁₋₁₄ (blue dotted line). Samples were prepared as 0.6 mM Cu^{II} and 0.7 mM HSA in 20 mM HEPES, or 2.0 mM Cu^{II} and 2.1 mM hCtr1₁₋₁₄ in 50 mM HEPES. Both samples were at pH 7.4.

Our results indicate that the ATCUN motif of the extracellular N-terminus of hCtr1 is the main anchoring site for Cu^{II} ions. It is strong enough to collect Cu^{II} from HSA, that carries the significant portion of exchangeable Cu^{II} in the blood.³¹ The Cu^{II} binding at this site is potentially the first step of copper import to the cell. Then, as shown previously, Cu^{II} bound to the N-terminus could be reduced to Cu^I by physiological reducing agents such as ascorbate^{8,5} or perhaps STEAP reductases^{32,33} to enable copper to move across the membrane, as in-principle hCtr1 is a Cu^I transporter. Our *in vitro* study therefore provides support for a mechanism of action of hCtr1 which includes direct transfer of Cu^{II} from extracellular copper carriers.

Conflicts of interest

There are no conflicts to declare.

Acknowledgements

The equipment used was sponsored in part by the Centre for Preclinical Research and Technology (CePT), a project co-sponsored by European Regional Development Fund and Innovative Economy, The National Cohesion Strategy of Poland. The study was financed by the Preludium grant, No. 2016/21/N/NZ1/02785, by Opus grant

No. 2016/23/B/ST5/02253, National Science Centre of Poland, and by the Frontier Research in Chemistry Foundation, Strasbourg (CSC-PFA-17). N. E. Wezynfeld was supported by Start Programme funded by Polish Science No. START 90.2017 and Mobility Plus Programme funded by Polish Ministry of Science and Higher Education No. 1632/MOB/V/2017/0. K.H. gratefully acknowledges support from a Research Corporation for Science Advancement Cottrell Scholar Award. Portions of this research were carried out at the Stanford Synchrotron Radiation Lightsource, a Directorate of SLAC National Accelerator Laboratory and an Office of Science User Facility operated for the U.S. Department of Energy Office of Science by Stanford University. The SSRL Structural Molecular Biology Program is supported by the DOE Office of Biological and Environmental Research, and by the National Institutes of Health, National Center for Research Resources, Biomedical Technology Program (P41RR001209).

References

- J. H. Kaplan and E. B. Maryon, *Biophys. J.*, 2016, **110**, 7–13.
- C. Cheignon, M. Tomas, D. Bonnefont-Rousselot, P. Faller, C. Hureau and F. Collin, *Redox Biol.*, 2018, **14**, 450–464.
- E. Carboni and P. Lingor, *Metallomics*, 2015, **7**, 395–404.
- C. J. De Feo, S. G. Aller, G. S. Siluvai, N. J. Blackburn and V. M. Unger, *PNAS*, 2009, **106**, 4237–4242.
- S. Schwab, J. Shearer, S. E. Conklin, B. Alies and K. L. Haas, *J. Inorg. Biochem.*, 2016, **158**, 70–76.
- S. Puig, J. Lee, M. Lau and D. J. Thiele, *J. Biol. Chem.*, 2002, **277**, 26021–26030.
- D. Kahra, M. Kovermann and P. Wittung-Stafshede, *Biophys. J.*, 2016, **110**, 95–102.
- K. L. Haas, A. B. Putterman, D. R. White, D. J. Thiele and K. J. Franz, *J. Am. Chem. Soc.*, 2011, **133**, 4427–4437.
- Y. Guo, K. Smith, J. Lee, D. J. Thiele and M. J. Petris, *J. Biol. Chem.*, 2004, **279**, 17428–17433.
- J. F. Eisses and J. H. Kaplan, *J. Biol. Chem.*, 2005, **280**, 37159–37168.
- M. J. Petris, K. Smith, J. Lee and D. J. Thiele, *J. Biol. Chem.*, 2003, **278**, 9639–9646.
- P. Gonzalez, K. Bossak, E. Stefaniak, C. Hureau, L. Raibaut, W. Bal and P. Faller, *Chem. Eur. J.*, 2018, **24**, 8029–8041.
- D. Płonka and W. Bal, *Inorganica Chim. Acta*, 2018, **472**, 76–81.
- M. Mital, N. E. Wezynfeld, T. Frączyk, M. Z. Wiloch, U. E. Wawrzyniak, A. Bonna, C. Tumpach, K. J. Barnham, C. L. Haigh, W. Bal and S. C. Drew, *Angew. Chemie - Int. Ed.*, 2015, **54**, 10460–10464.
- E. Georgatsou, L. A. Mavrogiannis, G. S. Fragiadakis and D. Alexandraki, *J. Biol. Chem.*, 1997, **272**, 13786–13792.
- M. C. Linder, *Metallomics*, 2016, **8**, 887–905.
- T. Z. Kidane, R. Farhad, K. J. Lee, A. Santos, E. Russo and M. C. Linder, *BioMetals*, 2012, **25**, 697–709.
- Y. Shenberger, A. Shimshi and S. Ruthstein, *J. Phys. Chem. B*, 2015, **119**, 4824–4830.
- M. Sendzik, M. J. Pushie, E. Stefaniak and K. L. Haas, *Inorg. Chem.*, 2017, **56**, 15057–15065.
- X. Du, H. Li, X. Wang, Q. Liu, J. Ni and H. Sun, *Chem. Commun.*, 2013, **49**, 9134–9136.

Journal Name

COMMUNICATION

- 1
2
3
4
5
6
7
8
9
10
11
12
13
14
15
16
17
18
19
20
21
22
23
24
25
26
27
28
29
30
31
32
33
34
35
36
37
38
39
40
41
42
43
44
45
46
47
48
49
50
51
52
53
54
55
56
57
58
59
60
- 21 M. Rózga, M. Sokołowska, A. M. Protas and W. Bal, *J. Biol. Inorg. Chem.*, 2007, **12**, 913–8.
- 22 K. Bossak, S. C. Drew, E. Stefaniak, D. Płonka, A. Bonna and W. Bal, *J. Inorg. Biochem.*, 2018, **182**, 230–237.
- 23 N. E. Wezynfeld, K. Bossak, W. Goch, A. Bonna, W. Bal and T. Frączyk, *Chem. Res. Toxicol.*, 2014, **27**, 1996–2009.
- 24 E. Kopera, A. Krezel, A. M. Protas, A. Belczyk, A. Bonna, A. Wyśtouch-Cieszyńska, J. Poznański and W. Bal, *Inorg. Chem.*, 2010, **49**, 6636–45.
- 25 A. E. M. Klomp, B. B. J. Tops, I. E. T. Van Den Berg, R. Berger and L. W. J. Klomp, *Biochem. J.*, 2002, **364**, 497–505.
- 26 J. A. Mindell, *Annu. Rev. Physiol.*, 2012, **74**, 69–86.
- 27 L. D. Pettit, S. Pyburn, W. Bal, H. Kozłowski and M. Bataille, *J. Chem. Soc. Dalton Trans.*, 1990, 3565–3570.
- 28 M. Sokołowska and W. Bal, *J. Inorg. Biochem.*, 2005, **99**, 1653–1660.
- 29 C. Hureau, H. Eury, R. Guillot, C. Bijani, S. Sayen, P. L. Solari, E. Guillon, P. Faller and P. Dorlet, *Chem. Eur. J.*, 2011, **17**, 10151–10160.
- 30 V. A. Streltsov, R. S. K. Ekanayake, S. C. Drew, C. T. Chantler and S. P. Best, *Inorg. Chem.*, 2018, **57**, 11422–11435.
- 31 E. L. Giroux and R. I. Henkin, *Bioinorg. Chem.*, 1973, **2**, 125–133.
- 32 D. Ramos, D. Mar, M. Ishida, R. Vargas, M. Gaite, A. Montgomery and M. C. Linder, *PLoS One*, 2016, **11**, e0149516.
- 33 R. S. Ohgami, D. R. Campagna, A. McDonald and M. D. Fleming, *Blood*, 2006, **108**, 1388–1394.